Upper and Lower Exoskeleton Limbs for Assistive and Rehabilitative Applications

Dasheek Naidu, Calvin Cunniffe, Riaan Stopforth, Glen Bright and Shaniel Davrajh

Mechatronics and Robotics Research Group- Bioengineering Unit
School of Mechanical Engineering
University of Kwa-Zulu Natal
Durban, South Africa
dasheekn@gmail.com, cunniffec@gmail.com, stopforth@ukzn.ac.za, brightg@ukzn.ac.za and sdavrajh@ukzn.ac.za

Abstract— Individuals with tetraplegia have loss of motor function in both their upper and lower extremities. Research is being conducted into the development of an exoskeleton to cater for the tetraplegic user. An exoskeleton system has the advantage of assisting disabled or rehabilitating patients without the need of surgery. This paper includes the conceptual design of an upper and lower limb exoskeleton which will be used for rehabilitative and assistive purposes. The mechanical design, kinematical analysis and control architecture will be outlined. Simulated results of the workspace were conducted for the specific design and kinematic models.

I. INTRODUCTION

The 21st century has seen the realisation of wearable robots. From their first introduction into the industrial workplace in the 1960s [1], robots have developed at an incredible rate and now encompass almost every aspect of modern society. Wearable robots are defined as "a mechatronic system that is designed around the shape and function of the human body, with segments and joints corresponding to those of the person it is externally coupled with" [2]. Due to technological developments, robotic exoskeleton systems have evolved from rudimentary prototypes with limited application to highly sophisticated devices. These systems have the ability to enhance the performance of humans and enable disabled individual to perform actions according to the Activities of Daily Living [ADL].

The exoskeleton structure in this paper is intended for individuals who have lost their motor functions in their upper or lower limbs. Damage to the central nervous system or spinal cord injuries may result in such a loss of upper or lower limb motor functions [3],[4]. There are approximately 12 000 new cases of spinal cord injuries per annum, with a total of over 250 000 cases in the United States of America alone [3]. Severe trauma to the spinal cord may result in paraplegia or tetraplegia. Paraplegia is the loss of motor function in the lower extremities; usually with retained upper limb functions. Such an injury could result in the implementation of the lower limb exoskeleton. Tetraplegia is the loss of both upper and lower limb motor functions [3]; this will require the implementation of both upper and lower exoskeleton devices.

The exoskeleton devices will be required to produce a workspace; which will replicate the spherical motion that represents the shoulder joint's mobility and in the case of the lower limb exoskeleton, permits standing and walking.
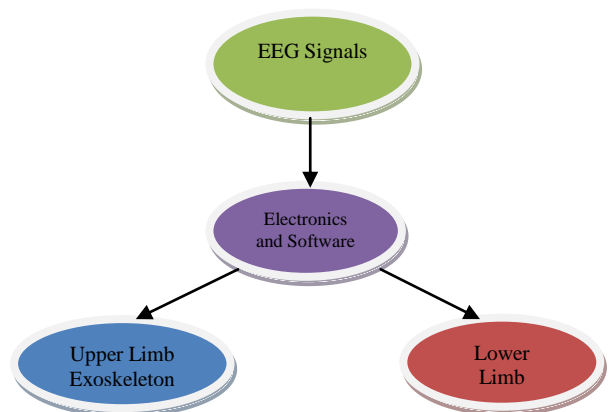

Fig 1: The implementation of the exoskeleton devices.

The content in this paper relates to the relevant exoskeleton designs. However, these exoskeletons are created such that it will allow for future implementation of an EEG (electroencephalogram) controlled system. Electroencephalography is the art of monitoring the brain's electrical activity. The brain consists of neural tissue, consisting of neurons among other matter. An electrical potential exists across the cells and varies depending on the stimulus. Electrical potentials at the cells can either sum up or cancel out, thus resulting in the overall brain activity which can be measured at the scalp [5]. These electrical potentials are received via electrodes positioned on the scalp for non-invasive data acquisition [6]. These potentials will act as an external input and is conceptualised in Fig 1.

A. Existing Exoskeletons

The concept of using an exoskeleton for protection or enhancement has been around for hundreds of years. However it was only until recently that powered exoskeletons became a reality. One of the first contributions to early development of

powered exoskeletons was 'HARDIMAN'. This full body exoskeleton was designed by General Electric co. in the 1960's, consisting of an inner and outer exoskeleton which operated on a master/slave control scheme [5]. In the last 5 years there has been major development in exoskeleton systems [2]. Systems such as the Hybrid Assistive Limb (HAL), which is now in the fifth generation, and Berkley's BLEEX, display cutting edge modern technology.

HAL-5 was designed by researchers at the University of Tsukuba, Japan. The HAL-5 was aimed at meeting both strength augmentation and rehabilitation requirements. HAL-5 is a full body exoskeleton which is controlled by two control schemes, namely "Bio-cybernetic control" and "cybernetic robot control" [7]. The former control scheme utilizes electromyography (EMG) signal detection for augmentation operation. The latter control scheme is used for repetitive activities or when there are no viable EMG signals. This draws on a database of predefined motions for a specific operator [8].

BLEEX is a lower limb robotic exoskeleton which was developed by researchers, at the University of California Berkley, in an effort to improve the load bearing capabilities of the operator. BLEEX is controlled through a highly sensitive control system which uses data from sensors on the exoskeleton to predict the movement of the operator. However, there are no sensors measuring the interaction force between the operator and the exoskeleton [9].

The L-EXOS was designed by PERCO situated in Italy. The L-EXOS is an upper limb exoskeleton which implements a drive pulley system. This pulley system allows for remote positioning of the actuators, thereby reducing the moments acting on the mechanical manipulator. The pulley actuation system is undesirable as it complicates the mechanism's ability to be adjustable; due to the constant tension required by the pulleys. The spherical motion is produced by orthogonal joints which result in a bulky system; therefore requiring a fixed external support. The L-EXOS was inspirational in terms of its implementation of serial joints which were required to produce a spherical motion. However, this orthogonal layout resulted in a bulky system [10].

The MGA exoskeleton was designed at the University of Maryland, for rehabilitative purposes and produces the desired spherical motion without the requirement of orthogonal joints. Individual joints were actuated by electric geared motors. The design does not implement a wrist or hand mechanism, and the links are bulkier than desired. It also consists of an additional degree of freedom for scapula motion which is not required in this research. The geared motors and the non-orthogonal requirement are implemented in this research [11].

The ARMin II was designed by the Swiss Federal Institute of Technology, Zurich, and is a rehabilitative exoskeleton that consists of the supination and pronation of the wrist. It actuates a steel cable which in turn rotates a semi-circular cuff. The cuff creates the required supination and pronation motion [12]. This wrist design will form the foundation of the wrist mechanism in this research.

II. MECHANICAL DESIGN

The mechanical designs of both the upper and lower exoskeletons will be illustrated in this section. The exoskeletons were designed to be anthropomorphic; therefore a basic understanding of the human anatomy is crucial.

The lower limb of the human skeleton comprises of three primary joints, namely the hip, knee and ankle. The degrees of freedom (DOF) each joint permits is illustrated in Fig 2 [7].
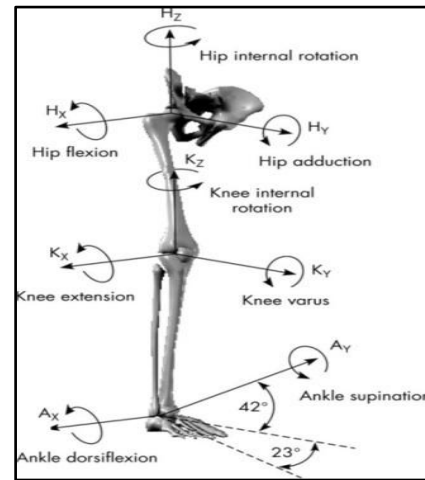

Fig 2: Lower limb degrees of freedom

Stability was neglected due complexity and funding restrictions. The operator's balance will be maintained through the use of stability aids, such as crutches.

Hip abduction/adduction and internal rotation do not play a significant role during the walking cycle [13], and were omitted from the design. A conceptual design was developed, as seen in Fig 3, which permitted walking in a straight line. This straight line walking means that the hip, knee and ankle joints permit articulation of the limbs in the sagittal plane.
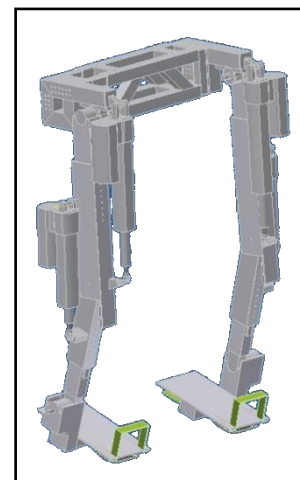

Fig 3: Lower limb conceptual design

Table 1: Joint range of motion

Joint	Motion	Human Maximum [5]	Walking Maximum [14]	Operational limitations
Hip	Flexion	120°	32.2°	90°
	Extension	-	22.5°	25°
Knee	Flexion	120°	73.5°	90°
Ankle	Flexion	50°	14.1°	20°
	Extension	20°	20.6°	15°
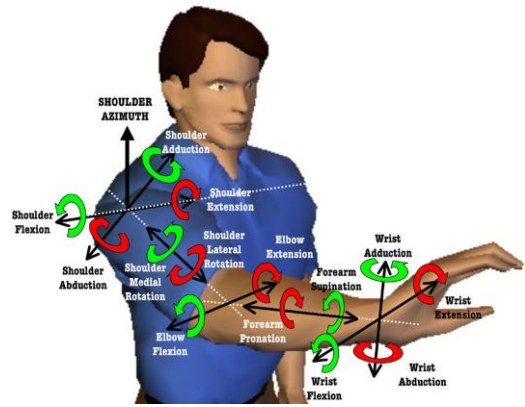
The ranges of motion for the joints are constrained such that hyper-extension and hyper-flexion do not occur. These ranges are tabulated in Table 1. Mechanical stops at the extremities act as a failsafe in the event of an electrical or software failure.

Both the hip and knee DOF were actuated, while the ankle joint was designed to be passive. A torsion spring mounted at the ankle was used to return the foot plate to a neutral position during the swing phase of the walking cycle. Data from Clinical Gait Analysis [15] were evaluated to determine the joint torques for the actuated DOF. For a 100 kg system, the torque requirement for hip extension was 80 Nm. The torque required for knee extension during stair climbing was 140 Nm and 50 Nm during walking. Actuators were selected such that the maximum torque was met, which allows for the operator to be raised or lowered from a seated position. Electric linear actuators from Phoenix Mecano's LZ60 range were selected as they offered high speed/load capabilities and a less bulky design than direct mounted rotational actuators.

There are 7 DOF in the human arm; of which three are represented by the glenohumeral (shoulder) joint. These three DOF contribute to the fundamental spherical motion of the exoskeleton arm, which is required to create a large workspace. Traditional upper limb exoskeletons implement three serial mutually intersecting orthogonal joints, which replicate the spherical motion created by the glenohumeral (GH) joint. However, this joint layout leads to a bulky design since the orthogonal joints have to be at a distance that avoids collision of the links with the human body. The elbow consists of one degree of freedom and produces an extension/flexion motion. The wrist consists of 3 DOF which includes the supination and pronation movements, illustrated by Fig 4 [11], along with the relative joint motions. Wrist abduction/adduction and extension/flexion was omitted from this research as it can be replicated by manipulating the three DOF which represent the GH joint.

Fig 4: Various joint motions in the human arm.

Inequalities (1) and (2) [11] are implemented to avoid the need for three mutual intersecting orthogonal joints. A spherical workspace will be achieved if the three serial joints which represent the GH joint are mutually intersecting, and satisfy the two inequalities. The origin of these inequalities can be found in [8].

$$\frac{\pi}{2} - \theta_3 \leq \theta_2 \leq \frac{\pi}{2} + \theta_3 \tag{1}$$

$$\pi - \theta_2 - \theta_3 \leq \theta_1 \leq \theta_2 + \theta_3 \tag{2}$$

θ_1, θ_2 and θ_3 are according to Fig 5 [11] and the tooltip represents the direction of the end-effecter. The upper limb exoskeleton was designed by implementing inequalities (1) and (2). The elbow mechanism was easily attached to the shoulder mechanism by adding an extra serial joint; this design can be seen in Fig 6 [Adapted from [16]]. θ_1, θ_2 and θ_3 are 90^0, 45^0 and 90^0 respectively in the design represented by Fig 5. The shoulder and elbow links are smaller and thinner than the MGA. This size reduction allows for easier connection to the lower limb exoskeleton as the manipulator is less bulky.
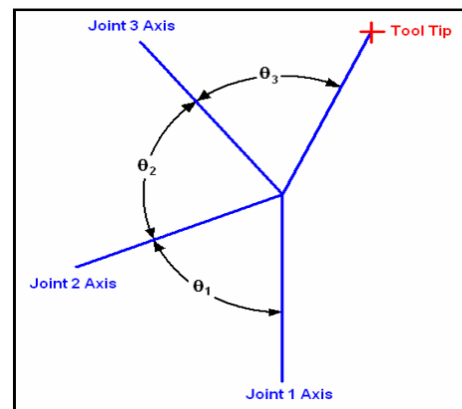

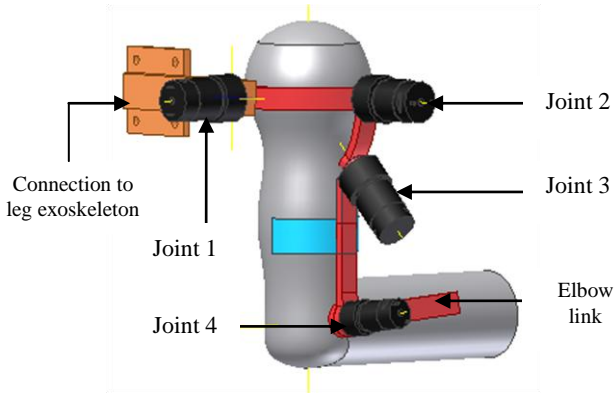Fig 5: Figure of the intersection of the GH joints and their relative angles.

Fig 6: CAD of the exoskeleton upper limb design.

The hand (end-effecter) and wrist mechanism will be connected to the elbow link; these designs can be seen in Fig 7 [16] (a) and (b) respectively. The hand will be connected to the wrist mechanism via A and B, and C and D in Fig 7.
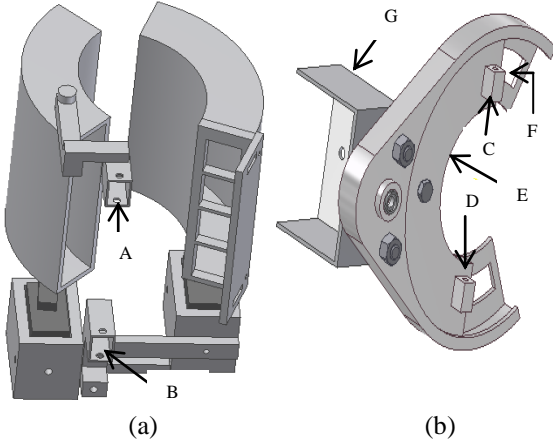

(a)   (b)

Fig 7: CAD of the exoskeleton hand (a), and wrist design (b).

The end-effecter exoskeleton allows for the placement of the thumb and the four fingers; providing the required gripping motion. The wrist design which is based on the ARMin II, will produce the above mentioned supination and pronation movements. It consists of a semi-circular gear which rotates in a slot and is actuated by a pinion gear that is powered by a DC motor. The wrist will be connected to the elbow link via connection point G (Fig 6). The slot and semi-circular gear (which will be strapped to the human hand) are represented in Fig 6 (b) by E and F respectively.

III. KINEMATICS ANALYSIS

A kinematics analysis was undertaken for both the upper and lower limb exoskeletons. The Denavit-Hartenberg (D-H)

convention was incorporated for assigning the reference frames. According to [1], the transformation matrix shown in (3), represents joint i relative to joint i-1. The exoskeletons are rigid serial mechanisms, which allows for the end-effecter to be represented relative to the fixed base frames [1].

a_{i-1} = distance from $\vec{z}_{i-1}$ to $\vec{z}_i$ about $\vec{x}_{i-1}$
α_i = angle from $\vec{z}_{i-1}$ to $\vec{z}_i$ about $\vec{x}_{i-1}$
θ_i = angle from $\vec{x}_{i-1}$ to $\vec{x}_i$ about $\vec{z}_i$
d_i = distance from $\vec{x}_{i-1}$ to $\vec{x}_i$ along $\vec{z}_i$

$$^{i-1}_iT = \begin{bmatrix} cos\theta_i & -sin\theta_i & 0 & \alpha_{i-1} \\ sin\theta_i cos\alpha_{i-1} & cos\theta_i cos\alpha_{i-1} & -sin\alpha_{i-1} & -d_i sin\alpha_{i-1} \\ sin\theta_i sin\alpha_{i-1} & cos\theta_i sin\alpha_{i-1} & cos\alpha_{i-1} & d_i cos\alpha_{i-1} \\ 0 & 0 & 0 & 1 \end{bmatrix} \quad (3)$$

The upper limb exoskeleton's transformation matrices are derived using the D-H method. These matrices are illustrated by (4)-(8) and will be used to derive the forward kinematics for the upper limb exoskeleton.

$$^0_1T = \begin{bmatrix} c1 & -s1 & 0 & 0 \\ s1 & c1 & 0 & 0 \\ 0 & 0 & 1 & 0 \\ 0 & 0 & 0 & 1 \end{bmatrix} \quad (4)$$

$$^1_2T = \begin{bmatrix} c2 & -s2 & 0 & 0 \\ 0 & 0 & 1 & 0 \\ -s2 & -c2 & 0 & 0 \\ 0 & 0 & 0 & 1 \end{bmatrix} \quad (5)$$

$$^2_3T = \begin{bmatrix} c3 & -s3 & 0 & 0 \\ s3.c\frac{\pi}{4} & c3.c\frac{\pi}{4} & -s\frac{\pi}{4} & -s\frac{\pi}{4}.L1.\sqrt{2} \\ s3.s\frac{\pi}{4} & c3.s\frac{\pi}{4} & c\frac{\pi}{4} & -c\frac{\pi}{4}.L1.\sqrt{2} \\ 0 & 0 & 0 & 1 \end{bmatrix} \quad (6)$$

$$^3_4T = \begin{bmatrix} c4 & -s4 & 0 & 0 \\ s4.c\frac{3\pi}{4} & c4.c\frac{3\pi}{4} & -s\frac{3\pi}{4} & -s\frac{3\pi}{4}.L1 \\ s4.s\frac{3\pi}{4} & c4.s\frac{3\pi}{4} & c\frac{3\pi}{4} & c\frac{3\pi}{4}.L1 \\ 0 & 0 & 0 & 1 \end{bmatrix} \quad (7)$$

$$^4_5T = \begin{bmatrix} c5 & -s5 & 0 & 0 \\ 0 & 0 & 1 & L3 \\ -s5 & -c5 & 0 & 0 \\ 0 & 0 & 0 & 1 \end{bmatrix} \quad (8)$$

L1 and L3 represent the distance from the GH joint to the elbow joint and the forearm length respectively. The forward kinematics of the exoskeleton arm were obtained using (9) [1]. This kinematics model relates the end-effector to the origin of the base frame, which is represented by the GH joint.

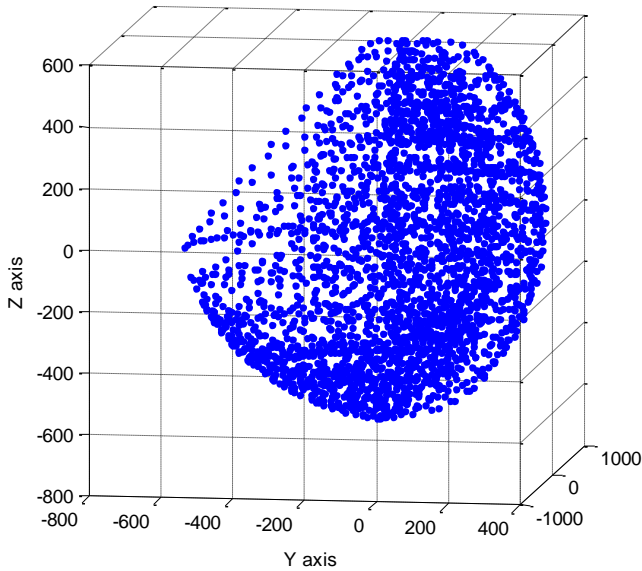$$^0_NT = {^0_1T}\,{^1_2T}\, ... \,{^{N-1}_NT} \quad (9)$$

Fig 8: Upper limb spherical workspace.

The first three rows of the last column of ^0_5T represent the X, Y and Z position of the end-effecter relative to the GH joint. Various end-effecter positions can be obtained by simulating a combination of different joint angles. Fig 8 is such a simulation and illustrates the spherical workspace achieved by the shoulder and elbow mechanism, with L1 and L3 set to 280 and 350 mm respectively. Therefore a successful exoskeleton shoulder design was created; as the three mutually intersecting joints created a spherical workspace. Such a device will enable individuals to carry out daily activities, due to the spherical motion, or rehabilitate patients by allowing joint angle repetition within the allowable workspace.

Both the lower limbs have identical kinematic chains, thus the fixed reference frame was defined at the hip, and the transformation matrices relating the ankle to the reference frame were found. These matrices can be seen in (11) - (13). The inverse kinematics were derived analytically and verified through simulations on Matlab ®. The workspace, seen in Fig 9 was programmed on Matlab ® using a random number generation method, and depicts the maximum range of motion for each leg. For simulation purposes limb lengths were set to 500 mm and 430 mm for the thigh and shank respectively.
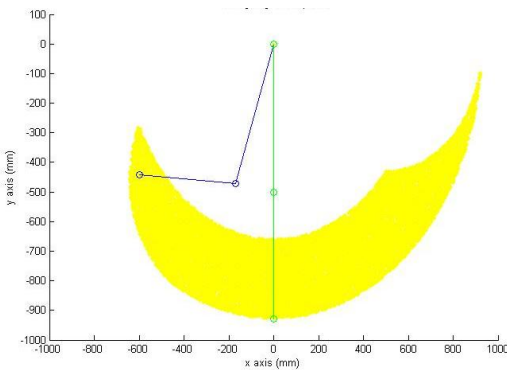

Fig 9: Range of motion for lower limbs.

The plane in Fig 9 represents the sagittal plane, with the anterior of the model facing the positive x direction. The workspace depicts the range of motion of the swing leg (blue), while the stance leg (green) is included for visual reference only. The full scope of the workspace includes the joint ranges both for motion while standing upright and in a seated position.

$$^0_1T = \begin{bmatrix} cos\theta_1 & -sin\theta_1 & 0 & 0 \\ sin\theta_1 & cos\theta_1 & 0 & 0 \\ 0 & 0 & 1 & 0 \\ 0 & 0 & 0 & 1 \end{bmatrix} \quad (11)$$

$$^1_2T = \begin{bmatrix} 1 & 0 & 0 & L_1 \\ 0 & 1 & 0 & 0 \\ 0 & 0 & 1 & 0 \\ 0 & 0 & 0 & 1 \end{bmatrix} \quad (12)$$

$$^2_3T = \begin{bmatrix} cos\theta_3 & -sin\theta_3 & 0 & L_2 \\ sin\theta_3 & cos\theta_3 & 0 & 0 \\ 0 & 0 & 1 & 0 \\ 0 & 0 & 0 & 1 \end{bmatrix} \quad (13)$$
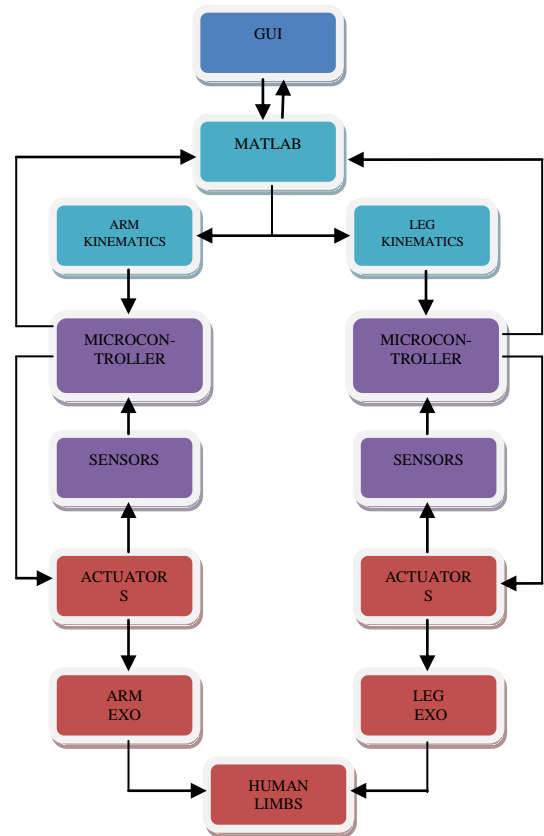
IV.   CONTROL ARCHITECTURE

Fig 10: Control architecture of the entire system.

The control architecture is in development. Instructions such as joint changes or co-ordinate points are provided via a graphics user interface (GUI). The data will be sent to Matlab ® which will carry out the relevant kinematic calculations. The calculated or inputted joint angles will then be sent to the relevant microcontrollers which will carry out the motor control operations, a well-established practice. Future implementation of the system will involve replacing or integrating the GUI, of the system illustrated in Fig 10, with a brain-controlled computer that will make use of an EEG.

V.   CONCLUSION

Both upper and lower exoskeleton designs were illustrated. The kinematic matrices were established for the relevant joint frames; these were used to determine the required kinematic models. The spherical workspace of the upper exoskeleton was established, as well as the workspace required to produce a successful lower limb. The mechanical concepts are therefore capable of performing rehabilitative and assistive contributions. The control architecture was outlined and the placement for a future brain-controlled device can be implemented.

[1]   J. J. Craig, Introduction to robotics: mechanics and control: Pearson/Prentice Hall, 2005.

[2]   S. Mohammed and Y. Amirat, "Towards intelligent lower limb wearable robots: Challenges and perspectives - State of the art," in Robotics and Biomimetics, 2008. ROBIO 2008. IEEE International Conference on, 2009, pp. 312-317.

[3]   H. M. Koslowski, "Spinal Cord Injury: Functional Outcomes in 2009 and Beyond," Northeast Florida Medicine, vol. 60, pp. 32-35, 2009.

[4]   N. I. o. N. D. a. Stroke. (2010, 31 May). NINDS Brachial Plexus Injuries Information Page. Available: http://www.ninds.nih.gov/disorders/brachial_plexus/brachial_plexus.htm

[5]   J. Pons, Wearable robots: biomechatronic exoskeletons: Wiley, 2008.

[6]   G. D. B. Blankertz, et al, "The Berlin Brain-Computer Interface: EEG-based communication without subject training," EnglishIEE Transactions on Neural Systems and Rehabilitation Engineering., vol. XX, pp. 1-6, 2006.

[7]   Y. Sankai, "Leading Edge of Cybernics: Robot Suit HAL," in SICE-ICASE, 2006. International Joint Conference, 2006, pp. P-1-P-2.

[8]   C. Inc. (2011, 18/05/2011). Hybrid Assistive Limb. Available:
http://www.cyberdyne.jp/english/index.html

[9]   H. Kazerooni, et al., "On the Control of the Berkeley Lower Extremity Exoskeleton (BLEEX)," in Robotics and Automation, 2005. ICRA 2005. Proceedings of the 2005 IEEE International Conference on, 2005, pp. 4353-4360.

[10]   F. R. A. Frisoli, et al... "A new force-feedback arm exoskeleton for haptic interaction in Virtual Environments," presented at the Proceedings of the First Joint Eurohaptics Conference and... 2005.

[11]   M. Liszka, "Mechanical Design of a Robotic Arm Exoskeleton for Shoulder Rehabilitation," University of Maryland, 2006.

[12]   T. N. a. R. R. M. Mihelj, "ARMin II-7 DoF rehabilitation robot: mechanics and kinematics," presented at the International Conference on Robotics and Automation, Roma, Italy, 2007.

[13]   K. Hian Kai, et al., "Development of the IHMC Mobility Assist Exoskeleton," in Robotics and Automation, 2009. ICRA '09. IEEE International Conference on, 2009, pp. 2556-2562.

[14]   A. Zoss, et al., "On the mechanical design of the Berkeley Lower Extremity Exoskeleton (BLEEX)," in Intelligent Robots and Systems, 2005. (IROS 2005). 2005 IEEE/RSJ International Conference on, 2005, pp. 3465-3472.

[15]   R. Riener, et al., "Stair ascent and descent at different inclinations," Gait & Posture, vol. 15, pp. 32-44, 2002.

[16]   D. Naidu, R. Stopforth, G. Bright and S. Davrajh, "A 7 DOF exoskeleton arm: shoulder, elbow, wrist and hand mechanism for assistance to upper limb disabled individuals," presented at the Africon, Zambia, 2011.